THE CALIBRATION OF AN AEROSOL CENTRIFUGE AND A STUDY OF DENSITY DEVIATION IN CONDENSATION AEROSOLS

A THESIS

Presented by

The Faculty of the Division of Graduate

Studies and Research

by

George Francis Boscoe

In Partial Fulfillment

of the Requirements for the Degree

Master of Science in Chemical Engineering

Georgia Institute of Technology

October, 1972

THE CALIBRATION OF AN AEROSOL CENTRIFUGE AND A STUDY OF DENSITY DEVIATION IN CONDENSATION AEROSOLS

Approved:

Chairman

Date approved by Chairman: 11-10-72

In presenting the dissertation as a partial fulfillment of the requirements for an advanced degree from the Georgia Institute of Technology, I agree that the Library of the Institute shall make it available for inspection and circulation in accordance with its regulations governing materials of this type. I agree that permission to copy from, or to publish from, this dissertation may be granted by the professor under whose direction it was written, or, in his absence, by the Dean of the Graduate Division when such copying or publication is solely for scholarly purposes and does not involve potential financial gain. It is understood that any copying from, or publication of, this dissertation which involves potential financial gain will not be allowed without written permission.

7/25/68

ACKNOWLEDGEMENTS

This work was supported in part by an Enviornmental Protection Agency Training Grant AP-00086-02. I express my gratitude to Dr. Othmar Preining and Dr. Michael Matteson for their encouragement during this study.

TABLE OF CONTENTS

Page

ACKNOWLEDGMENTS iii

LIST OF TABLES vi

LIST OF ILLUSTRATIONS vii

SUMMARY viii

Chapter

I. INTRODUCTION 1

II. INSTRUMENTATION AND EQUIPMENT 6

Aerosol Centrifuge
Centrifuge Calibration Equipment
Aerosol Generator

III. PROCEDURE 14

Centrifuge Calibration
Sodium Chloride Aerosol Analysis

IV. RESULTS 17

Calibration of the Aerosol Centrifuge
Particle Characteristics
Relationship of Aerodynamic Diameter to Particle Mean Density
Relationship of Particle Density at Constant Temperature to Flow Rate
Relationship of Particle Density at Constant Flow Rate to Temperature
Error Analysis

V. CONCLUSIONS 33

VI. RECOMMENDATIONS 35

APPENDIX

A. Aerosol Centrifuge Calibration Data 37

B. Tabulation of Experimental Results of Sodium Chloride Aerosol Density Analysis 39

Table of Contents (Continued)

Page

C. The Derivation of the Pressure Drop Expression Through the Centrifuge Orifice and Calculation of the Average Annular Gas Velocity in the Annular Channel 50

D. Comparison of Sedimentation Length Functions 54

E. Nomenclature 58

LITERATURE CITED 60

LIST OF TABLES

Table		Page
1.	Calibration Particle Parameters	8
2.	Relative Aerodynamic Size of Aggregates of Uniform Spheres	18
3.	Calibration Data for Aerosol Centrifuge	37
4.	Sodium Chloride Aerosol Analysis Data	39
5.	Comparison of Experimentally Measured and Calculated Gas Flow Through Centrifuge Orifices	53
6.	Calculated Sedimentation Distance for Different Orifices	57

LIST OF ILLUSTRATIONS

Figure		Page
1.	Modified Aerosol Centrifuge	10
2.	Orifice Calibration Device	11
3.	Experimental Apparatus for Centrifuge Calibration	12
4.	LaMer-Sinclair Condensation Aerosol Generator	13
5.	Centrifuge Calibration Diagrams	20
6.	Sodium Chloride Particles	25
7.	Particle Density as a Function of Aerodynamic Diameter	26
8.	Cumulative Plot of Aerosol Particle Densities	27
9.	Particle Density as a Function of Flow Rate	29
10.	Particle Density as a Function of Temperature	30

SUMMARY

The research in this thesis is divided into two sections; the calibration of an aerosol centrifuge with a study of the fluid flow problems therein and the study of density deviation of sodium chloride condensation aerosols.

The use of well defined monodispersed aerosols is essential for calibration of particle sizing instruments and for laboratory experiments. Researchers have historically used optical methods and assumed bulk density in order to calculate the aerodynamic diameter of aerosols. The density of sodium chloride condensation aerosol particles in the range of 0.5 μm to 1.5 μm has been found to deviate from the bulk density as a function of the temperature and the flow rate in the primary heater of a LaMer generator. Future calculations using aerodynamic diameters of condensation aerosols should consider the effect of generator parameters on particle density.

An expression has been derived for the sedimentation distance in a cylindrical annular flow aerosol centrifuge and the results compare well with experimental data obtained by calibration of the centrifuge using polystyrene latex spheres. The design of other types of aerosol centrifuge is now possible using the sedimentation equation derived herein.

CHAPTER I

INTRODUCTION

The purpose of this research is twofold: to calibrate a modification of a recently designed aerosol centrifuge and to apply the centrifuge quantitatively to measure density distributions in sodium chloride aerosols formed by condensation in a LaMer-type generator. The influence of temperature and residence time in the generator on aerosol density is to be assessed.

For the calibration of particle sizing instruments and for laboratory experiments, the use of well defined monodispersed aerosols is essential. Sinclair and LaMer (1) developed condensation, sodium chloride, aerosol generators for light scattering studies. Until now it has been generally assumed that the aerosol particles generated by these devices had the same density as the bulk material from which they were formed. Recent experiments have proven, however, that particle densities are different from the bulk density of sodium chloride (2). It is suspected that the monodispersed, spherical, condensation aerosol which is generally measured by light scattering techniques is really a conglomeration of smaller loosely bound particles.

At a constant flow rate in the primary furnace, the effect of raising the temperature should be to increase the density of each aerosol particle because the vapor concentration would be higher. At a constant temperature in the furnace, the effect of increasing the flow rate should be to decrease the density of each particle because the

vapor concentration would be lower. Sinclair (1) demonstrated that optically larger aerosol particles are formed at the higher temperatures and flow rates. Also the surface tension of sodium chloride controls the formation of the final aerosol particles for they are normally spherical in shape.

Recently Moss (3) has confirmed by the use of a modified, Stober-type, aerosol centrifuge that the density distribution of fly ash and iron oxide particles is independent of particle size and is essentially the same as the bulk density of the material. Moss's investigation was conducted because of findings that very large particles of iron oxide (50μm) appeared to be hollow when viewed with an electron microscope.

Matteson, et al., (2) found the densities of fine particles of sodium chloride in the size range 0.05-0.35 μm to be between 0.2 gm/cm^3 and the bulk density of sodium chloride, 2.16 gm/cm^3 (4).

Stein et al., (5) found the density of uranine particles generated by a Dautrebande generator was 0.58 gm/cm^3. The density of the bulk material is reported by Fisher Scientific Company to be 1.53 gm/cm^3. Stein proposed no mechanism for this apparent discrepancy. Tillery (6) and Sehmel (7) in separate articles challenged Stein's findings and pointed out the density deviation was due to the method which Stein used to produce his final aerosols, that of drying them at an elevated temperature.

In this study of density distribution it was decided to compare the aerodynamic diameter with the optical or observed diameter of a monodispersed sodium chloride aerosol sampled in a modified Hochrainer (8) type aerosol centrifuge (HMC) and generated in a Sinclair-LaMer type

generator (SLG).

The aerodynamic diameter (DAE) is defined as

....."the diameter of a sphere of unit density which in a force field assumes the same steady state velocity as the actual particle under consideration". (8)

From Stokes' law*:

$$V_S = \frac{(DO)^2 \rho g C}{18 \mu} \qquad (1)$$

The correction factor, C, is not necessary for large particles and is not of primary importance unless the particle diameter approaches the mean free path length of the molecules of the carrier gas. The density of a particle is then given by the expression:

$$\rho = \left[\frac{DAE}{DO}\right]^2 \qquad (2)$$

The rationale was first to calibrate the aerosol centrifuge with monodispersed latex spheres of known size from the Dow Chemical Company**. By then measuring the sedimentation distances of the sodium chloride particles in the centrifuge, the aerodynamic diameter could be determined. The optical diameters (DO) were obtained by electron microphotography. Once these values were had, the density was easily calculated from Equation 2.

Hochrainer (8) developed an aerosol centrifuge which is quite simple in design and inexpensive to construct. It was from Hochrainer's model that the centrifuge of this thesis was developed. Hochrainer calibrated his centrifuge using Dow monodispersed latex spheres and measured

*See Nomenclature, Appendix E, page
**Dow Chemical Company, Midland, Michigan.

their sedimentation distance to get a calibration function. In order to calculate a sedimentation distance in his model, Hochrainer made several important assumptions:

1. Radial particle velocity is controlled by centrifugal force and for spherical particles by the Stokes-Cunningham correction to Stokes' law.

2. Gas flow is uniform in the annulus.

3. Since Coriolis forces are negligible, the particle velocity in the rotational direction will be identical to the gas velocity.

Hochrainer developed the following equation to determine the deposition lengthsin the channel:

$$Z = \frac{9\,\eta\,Q}{2\pi^2 ah(DAE)^2\rho\omega^2\left[\frac{1+2A\lambda\sqrt{\rho}}{DAE\sqrt{\rho}}\right]} \qquad (3)$$

From his experimental results in determining the sedimentation distance, Hochrainer found the flow rate, Q, in the centrifuge. In this thesis theoretical sedimentation distances were calculated from experimental values of the flow rate measured independently and then compared with experimental results.

The centrifuge used in this research was designed from Hochrainer's model. Several changes were made and tested. The aerosol channels in the original design were slits, this gave a broad band deposit of aerosol on the collecting strip. Here a small circular channel was used which made the aerosol deposit appear as a dot. It was also significantly simpler to build.

Most aerosol measuring devices developed today are calibrated with Dow polystyrene latex spheres. Dow provides latex spheres in sizes

between 0.09 and 3.5 μm in an aqueous suspension in concentrations between three and ten percent solids with a stabilizing agent. With each sample the manufacturer supplies data as to the mean diameter and standard deviation obtained by electronmicroscopy. The density of the aerosol particles after they are dried and suspended varies between 1.01 and 1.03 gm/cm^3.

CHAPTER II

INSTRUMENTATION AND EQUIPMENT

The description of the equipment will be divided into three parts; the aerosol centrifuge, the centrifuge calibration apparatus, and the aerosol generator.

Aerosol Centrifuge

The aerosol centrifuge was composed of three pieces; an aluminum outer casing, a brass cover and foil holder, and an inner brass rotor (Figures 1 a-d). The centrifuge was mounted in the chuck of a Stanley*, 1/4 hp, high-speed, router motor, Model No. 91014, which was connected to a rheostat and a Sola** constant voltage transformer Model 23-22-150. The rheostat set at approximately 56 volts gave a centrifuge speed of 10,000 RPM. The speed of the centrifuge was measured with a General Radio*** Strobotac, Model 1538-A, strobe light. With manual control of the rheostat, the rotation speed could be held constant, and, when left unattended, the rotation speed would not fluctuate more than 50 RPM.

Aerosol entered the centrifuge through a channel in the top center by either flooding the entire top surface with aerosol or inserting a lance into the center hole. An advantage of the lance method was the reduction of atmospheric contamination, and losses prior to collection. The aerosol then traveled radially outward through two circular channels

*The Stanley Works, New Britain, Conn.
**Sola Electric Company, Elk Grove Village, Illinois.
***General Radio Corporation, Concord, Mass.

with openings spaced 180° from each other on the inner surface of the annulus. The larger channel had a diameter equal to the height of the annular channel, and when the aerosol left this channel it was deposited on a random basis on the outer wall of the annular channel. The purpose of this channel was to purge the air stream of all aerosol particles and then use it as a carrier gas for the aerosol issuing from the other, smaller channel. When the air, which was in laminar flow, had traveled around the channel the smaller stream was superimposed upon it and the particles which the latter stream contained were separated discretly according to aerodynamic diameter on the outer wall of the annulus. The air stream moved out of the centrifuge through an exit orifice which controlled the flow rate. The air was prevented from returning to the site of the large channel by a baffle placed between the large channel opening and the exit orifice.

Aerosol was deposited on an aluminum foil strip mounted so that the deposition location could be measured optically. The deposition location was a function of the angular velocity of the centrifuge, the carrier gas flow rate in the channel, and the aerodynamic diameter of the particles.

Orifices of the centrifuge were calibrated by placing them in a tube shown in Figure 2. A calculation was performed (see Appendix C) to determine the pressure drop across the orifice; from this the flow rate was determined. The orifices were experimentally calibrated to confirm the orifice coefficient, which was assumed to be 0.61.

Centrifuge Calibration Equipment

The centrifuge was calibrated with polystyrene latex spheres purchased from the Dow Chemical Company. Table 1 gives the sizes used to calibrate the centrifuge.

Table 1. Calibration Particle Parameters

Particle Diameter (μ)	Standard Deviation (μ)	Run Number
1.305	0.0055	LS-1166B
1.10	0.0043	LS-1199B
0.822	0.0016	LS-1020E
0.577	0.0022	LS-1018E
0.481	0.0158	LS-464E
0.312	0.0060	LS-057A

The latex spheres are marketed in a ten percent aqueous solution. In order to get the proper aerosol concentration, a trial and error method was used in nebulizing the suspension. The best aerosols were generated by nebulizing a 40:1 dilution of the original Dow solution in a No. 40 DeVibiss* glass nebulizer with air at a 0.835 Kg/cm^2 pressure drop across the nebulizer jet. The gas flow rate measured using the apparatus was 7.4 liters/minute.

The aerosol was dried by mixing it with ten liter/minute of dry air which had been passed through a silica gel column (see Figure 3). The two gas streams were obtained by passing air at 6.95 Kg/cm^2 regulated by needle valves through separate Millipore filters** with 0.22 micron pore size. The drying gas and aerosol were mixed in a 600 cm^3 glass tube prior to being fed to the aerosol centrifuge.

*DeVilbiss Company, Somerset, Pa.
**Millipore Filter Corporation, Bedford, Mass.

Aerosol Generator

The aerosol generator was of the LaMer type and is detailed in Figure 4. Reagent grade sodium chloride was placed in a porcelain boat which was in turn placed in a 2.18 cm I.D. McDaniels* high temperature combustion tube within the first heater, a Hoskins** electric furnace, Model 5A11OU. The temperature in the first heater was controlled by a Brown*** electric pyrometer, Model 1GB. Dry nitrogen monitored through Matheson**** R-6-15 Series, flow meters was used as the carrier gas. The flow was laminar at all times, and the gas stream was diffused by glass wool as it entered the tube.

The vaporized sodium chloride passed down the channel to a second heater similar to the first held constant at 870 °C. The temperature was controlled by a Wheelco*****, Model 192, electric pyrometer. The sodium chloride was revaporized in the second heater.

The aerosol then passed down the ceramic tube where the particles grew by condensation. The outside of the tube was wrapped with a copper-tube, water jacket and was also cooled by a Rotron******, Model 1600 electric fan blowing across the tube. The final aerosol was led to an OWL (10), built for the purpose of viewing the Tyndall spectra. The monodisperse aerosol was then fed to the centrifuge for calibration.

---

*McDaniels Refractory Porcelain Co., Beaver Falls, Pa.
**Hoskins Manufacturing Co., Detroit, Michigan.
***Brown Instrument Company, Philadelphia, Pa.
****Matheson Gas Products Co., East Rutherford, N.J.
*****Wheelco Instruments Division, Rockford, Illinois.
******Rotron Manufacturing Co., Woodstock, New York.

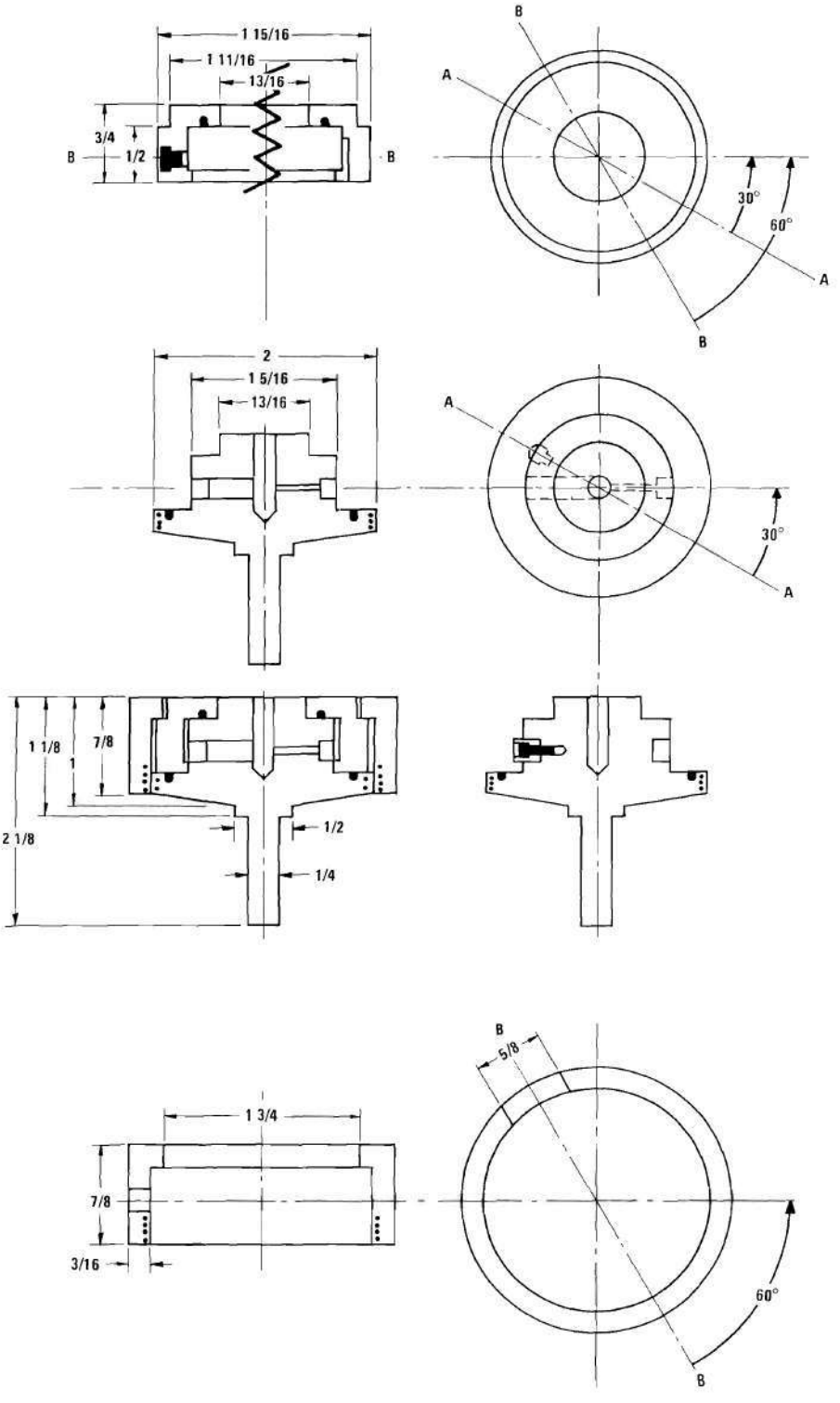

Figure 1. Modified Aerosol Centrifuge

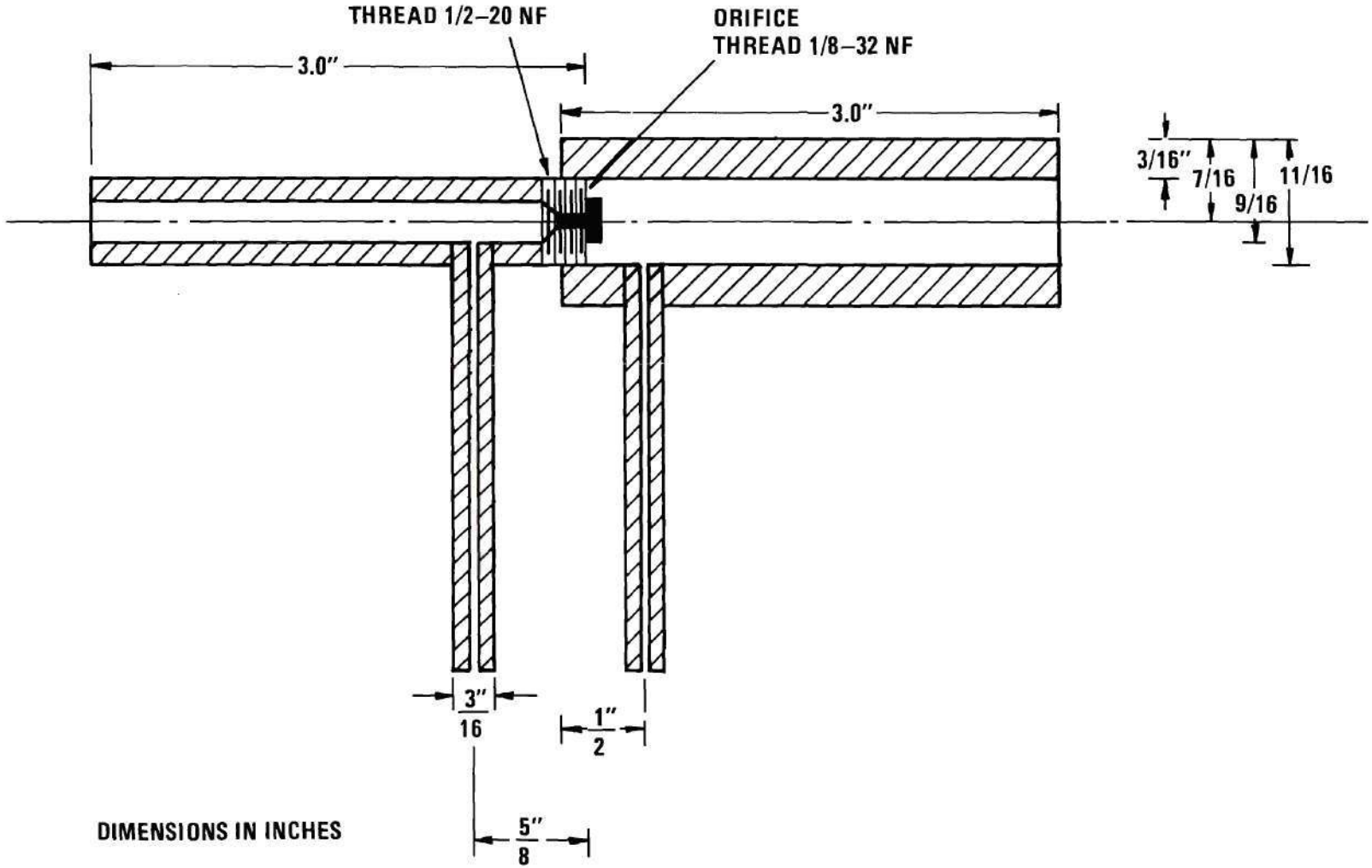

Figure 2. Orifice Calibration Device

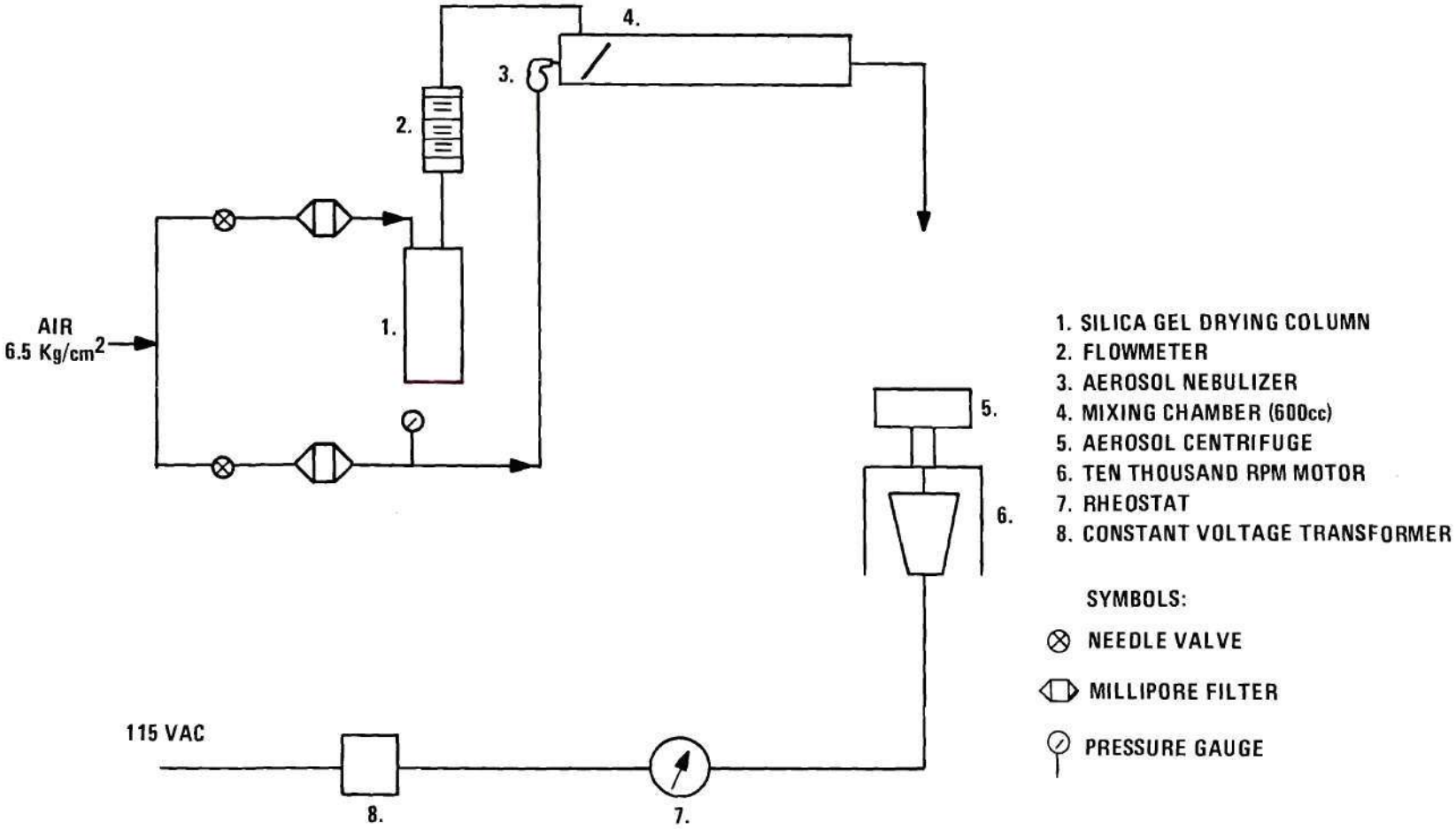

Figure 3. Experimental Apparatus for Centrifuge Calibration

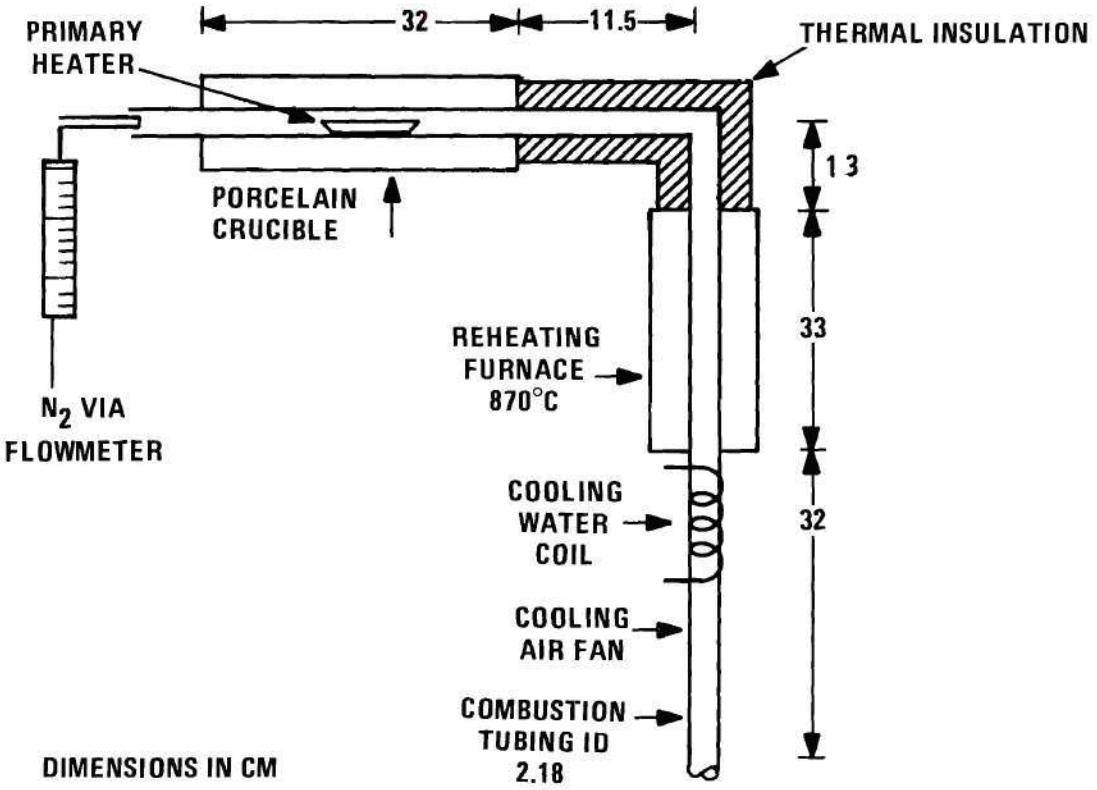

Figure 4. LaMer-Sinclair Condensation Aerosol Generator

CHAPTER III

PROCEDURE

Centrifuge Calibration

Dried aerosols from different sizes of polystyrene latex were injected into the centrifuge operating at 10,000 RPM for all experiments. An aluminum foil strip 1 cm x 4 cm was placed on the outer wall of the annular channel of the centrifuge where the aerosol was to be deposited. The orifices were also varied, and a calibration curve was obtained for each orifice.

Once the foil had the aerosol deposited upon it (after a sampling time of about twenty minutes) the samples were analyzed under a microscope with a ruler to find the mean deposit length for each particle size. This information was plotted on log-log coordinate graph paper (Figures 5a-d).

In order to compare the experimental deposit length with a calculated deposit length, the flow rate in the annulus had to be determined experimentally. Hochrainer (8) calculated the flow rate in his centrifuge from experimentally measured deposition lengths. It is proposed in this thesis that the exit orifice is the controlling factor in the flow rate, and, if the pressure drop across the orifice is known, the flow rate can be calculated and compared with experimental results.

Each orifice was calibrated by placing it in the pipe as shown in Figure 2 with the two taps connected to an inclined water gauge. A full range of pressure drops versus flow rates was measured for each orifice,

and the experimental values were compared with the theoretical values obtained using the orifice meter equation 4-117 from Coulson and Richardson (9).

Sodium Chloride Aerosol Analysis

The two heaters in the aerosol generator were controlled by resistance pyrometers. The first heater which controlled the rate of sodium chloride aerosol production was manipulated as was the flow rate of dry nitrogen through the generator.

Temperatures in the primary heater were varied from 843.6°C to 898.9°C and the flow rate was varied from 500 cc/min. to 1500 cc/min. This narrow range of conditions was necessary to obtain aerosols which were suitable for measurement within the calibration limits of the centrifuge.

The aerosol generator was operated until an optically monodispersed aerosol was obtained as outlined by Green and Lane (10). Since different flow rates and temperatures caused different amounts of aerosol to be formed, the samples exhibited different area concentrations on the foil.

Once the sodium chloride samples were collected they were immediately dessicated and prepared for study with the scanning electron microscope (SEM). To prepare the samples for the SEM, they had to be mounted on aluminum plates 5. mm x 12.5 mm. The length of the leading edge of the foil to the beginning of the deposit was measured and the foil was then cut and mounted to fit the small plates. These samples were taken to the SEM at the Georgia Institute of Technology Engineering Experiment Station where they were placed under a high vacuum and covered

with a fine layer of a gold-palladium alloy. The samples were viewed at various magnifications to determine the numerical frequency and optical diameter as a function of length on the small plate.

The ratio of the square of the aerodynamic diameter found from the deposition location in the aerosol centrifuge to the square of the optical diameter found from SEM studies yields the density of the particle.

Sodium chloride was chosen as the test aerosol primarily due to its ease of handling and availability. The major drawback to the use of sodium chloride as a condensation aerosol was the particles are spherical in shape when formed but rapidly formed cubic crystals if exposed to water vapor in the atmosphere for any length of time. This problem was greatest on days of high humidity.

CHAPTER IV

RESULTS

Calibration of the Aerosol Centrifuge

There were four orifices used to calibrate the centrifuge. An aluminum foil strip was placed on the outer wall of the annular channel to collect the polystyrene latex aerosol particles. The foils were mounted on microscope slides for examination and the sedimentation distances for the various singlets, doublets, and triplets were measured.

Preining (*11*) observed multiple aggregates of spheres of diameter 0.5 μm or less when testing aerosols generated from liquid suspensions by a nebulizing process. The formation of these aggregates can only be reduced by further diluting the liquid suspension, but excessive dilution of the suspension leads to many drops having no particles. This has the effect of reducing the particle concentration in the aerosol.

Stober (12) found the relative aerodynamic diameter for aggregates of particles with up to eleven particles in the mass. These numbers are presented below and were used as shown in Table 3 to determine the calibration curves for the centrifuge.

Table 2. Relative Aerodynamic Size of Aggregates of Uniform Spheres (11)

f(N)	Most Acceptable Value for DAE
f(2)	1.18
f(3)	1.33
f(4)	1.46

Microscopic analysis of the deposits on the foil clearly showed the presence of multiple aggregates. These aggregates were then assigned diameters according to their number from Table 2. An attempt was made to determine if a first-order relationship existed between the sedimentation distance and the particle diameter since a first-order least squares approximation fit the experimental data very well. Although the first-order approximation can be made to fit the experimental data, in theory the equation is unuseable because it predicted sedimentation distances for very small particles which are physically unrealistic. The calibration curves are presented in Figures 5a, b, c, d. Theoretical sedimentation distances are also presented on these curves.

A theoretical derivation of the sedimentation distance is presented in Appendix D. The basic assumptions involved are:

1. The exit orifice of the centrifuge controls the gas velocity through the annular channel.

2. The radial pressure drop through the orifice is a function of the centrifuge speed and design and the thermodynamic parameters of the gas but not the gas flow rate.

3. The radial motion of the particle is independent of its annular motion.

4. The equation is solved assuming no secondary flow in the

centrifuge.

These assumptions are made in addition to those proposed by Hochrainer (8) and reported in Chapter 1.

The results of the experimental calibration of the 0.0406 cm and 0.0508 cm orifices show that their flow rates are nearly identical. The calibration curves for aerosol sedimentation are also very nearly identical. The interpretation of these two results obtained independently of each other seems to point to the fact that the gas carrier velocity in the annular channel is a function of the exit orifice diameter. If the orifices are machined in such a way that they behave similarly under calibration testing, then they will yield nearly identical calibration curves. According to Coulson and Richardson (9) an orifice plate should be carefully drilled so that the edges are sharp. The orifices should have a low length-to-diameter ratio. The orifices built for the centrifuge considered herein were built by drilling a series of 3.2 mm diameter brass plugs to the desired diameter. The depth of the plugs was also 3.2 mm. The smaller orifices were built by partially drilling the holes with a 0.0508 cm drill and then finishing the hole with the desired size. This was done because the very small drills could not bore through a thick piece of metal.

These plugs were not true orifices in the sense described by Coulson (9) earlier. When a theoretical calculation to determine the flow rate through the orifice was performed for a compressible gas using Coulson and Richardson's equation

$$Q = .61\ \rho g A_o \sqrt{-2\rho g \Delta P} \qquad (4)$$

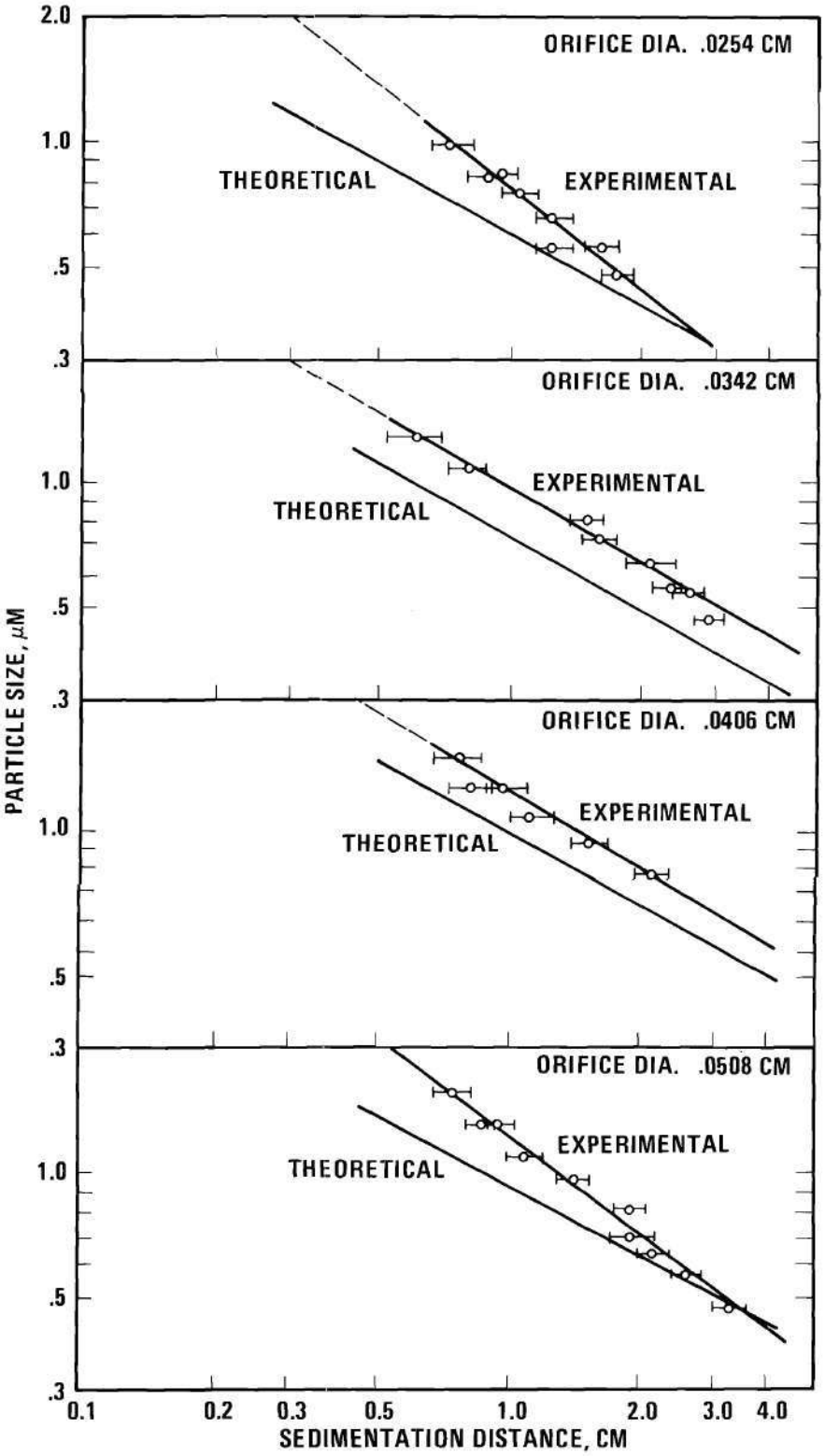

Figure 5. Centrifuge Calibration Diagrams

the results did not correlate well with the experimental data taken using the apparatus in Figure 2. It was assumed that the departure from theoretical values was due to poor orifice design. For this reason, values for annular average velocities were always obtained from the calibration data of the orifices and not from Equation 4.

To arrive at a theoretical expression for pressure drop across the orifice in the centrifuge a derivation is presented in Appendix C the result of which is

$$\frac{P}{P_o} = \exp\left(\frac{R^2 \omega^2 M}{2R'T}\right) \tag{5}$$

The equation clearly shows that the pressure drop across an orifice mounted on the centrifuge is independent of both flow rate and orifice diameter, and depends only on the distance from the center of the centrifuge to the orifice, R.

The pressure drop across the orifices for this centrifuge was 1695 dynes/cm^2. This result was derived assuming the temperature to be 300°K and the carrier gas to be pure nitrogen. Pure nitrogen was used as the carrier gas for the sodium chloride aerosol.

Using Goldstein's (13) equation which describes the velocity profiles in an annular channel for two dimensional flow in combination with an expression for the radial velocity, the following equation

$$Z = \left[\frac{\frac{(b-a)\bar{W}}{\frac{b^2-a^2}{4} - \frac{a^2b^2}{b^2-a^2}(\log b/a)^2}}{\frac{(DST)^2\omega^2}{18\mu}\left(\frac{1}{1+\beta x} + \frac{2.25x}{\delta}\right)}\right]\left[\frac{b^2\log b - a^2\log a}{(b^2-a^2)}\, a\left(\frac{b}{a}-1\right) + \frac{ab^2}{b^2-a^2}\log\frac{b}{a} + \ldots\right.$$
$$\left.\ldots a\left(\frac{b}{a}-1\right) - a\left[\frac{b}{a}\left\{\log\frac{b}{a} - 1\right\} + 1\right]\right] \tag{6}$$

is derived (Appendix D) which predicts the sedimentation distance for a particle in a centrifugal force field in an annular channel. It includes the Fuchs-Stechina correction to Stokes law (14).

A comparison was made of the sedimentation distances predicted from equation 6 and experimental results given in Table D-1 and Figures 5a, b, c, d. The experimentally derived sedimentation distances and theoretical distances calculated correlate well and support the assumptions made. All mean velocities ($\bar{W}$) were taken from the experimental results.

Particle Characteristics

The actual photomicrographs taken of the sodium chloride aerosol deposits were analyzed with a Zeiss* Particle Size Analyzer, Model TGZ3. Besides the frequency and optical diameter information, the photographs revealed other interesting properties of the aerosol particles.

Sodium chloride condensation aerosols as produced in a LaMer-type generator appeared as amorphous spherical masses. A very small amount of water vapor was found to cause crystallization of the particles into the classical cubical structure. Even though care was taken to keep the samples dessicated, some of them did crystallize. The crystallization took place after the particles had deposited on the aluminum foil collecting strip and not while they were in the gas stream, since the gas stream was dry nitrogen and the system was sealed from the atmosphere until the actual injection of the aerosol into the centrifuge. The crystallized aerosol samples were used as part of the data to determine particle density for two reasons. First, if the particles crystallized on the foil and not in the gas stream then only the optical

*Carl Zeiss, West Germany.

diameter would be affected in determining the density. And second, the crystallized samples used as data exhibited particles with rounded edges and some spherical particles which had not crystallized. It should be mentioned that the standard deviation of the particle sizes was much greater in the samples of crystallized particles than in those samples which were not crystallized.

It was noticed in some of the samples that particles with two different optical diameters were present. The differences in optical diameters were of such a magnitude that a straightforward calculation of particle densities would yield a bimodal distribution of particles with density differences on the order of 100 fold. The explanation for the presence in a deposit of very small particles can be given by returning to the design of the aerosol centrifuge used to collect the particles. Very small particles - those with sedimentation distances on the order of 7 to 9 cm would not be purged from the gas stream of the first large channel and would continue on around to settle at the same location as larger particles issuing from the smaller channel. From the calibration curves, Figures 5a-d, it can be seen that the smaller particles are on the order of 1000 Å units in diameter.

In general, the density of the aerosol particles was less than the bulk density of the parent material. The degree of deviation was definitely affected by the formation parameters in the aerosol generator. The fact that the density of condensation aerosols is different from the parent material may significantly affect results obtained in experiments where the dynamic properties of particles are studied.

When the aerosol particles were highly magnified the phenomena of

clustering could be seen. The surface of the particles appears rough and irregular in shape. Small bulges could be seen protruding from the sides of the particles. The most striking example of clustering can be seen in Figure 6 in the sample which has an aerodynamic diameter of 1.09 μm.

Relationship of Aerodynamic Diameter to Particle Mean Density

It was found that there exists a relationship between the aerodynamic diameter and the mean density of the sample. Figures 7 and 8 show that as the particle size decreases the departure of the density of the particles from the bulk density increases.

A second-order, least-squares calculation was made to determine an empirical relationship between the aerodynamic diameter and the mean density of the sample as shown in Figure 8. The result is given below

$$\bar{\rho}_{\substack{871^{o}C \\ 500\ cc/min}} = -.890 + 5.07\ (DAE) + 2.5\ (DAE)^{2} \qquad (7)$$

Several concepts should be kept in mind if an attempt is made to use this correlation. First, it is most probably good only for the specific instrument used in this research; also, it is only valid at the temperature and flow rate described; and the theoretical basis given to substantiate the order of correlation is equation 2.

Relationship of Particle Density at Constant Temperature to Flow Rate

Assuming that the density deviations found in condensation aerosols were caused by a mechanism described by the agglomeration of critical clusters of nuclei, an increase in flow rate through the system should reduce the vapor concentration coming from the first heater and reduce the time in the reheater.

An increase in the flow caused a decrease in the aerodynamic

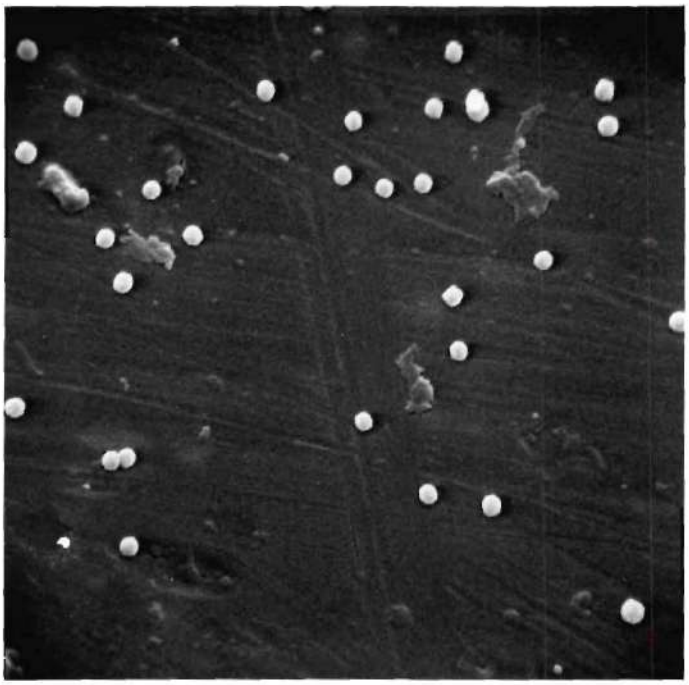

D_{St} = 0.702 μm

$\bar{\rho}$ = 1.25 gm/cm^3

D_{St} = 0.820 μm

$\bar{\rho}$ = 1.40 gm/cm^3

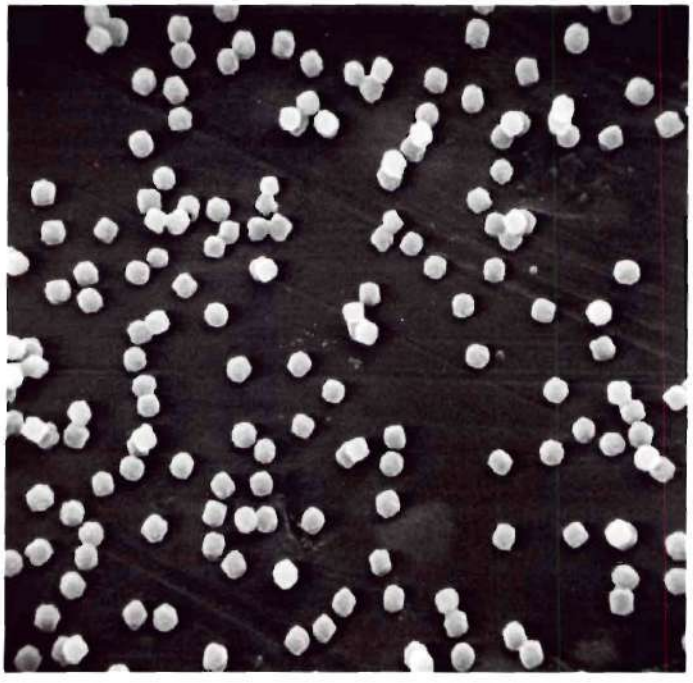

D_{St} = 0.960 μm

$\bar{\rho}$ = 1.50 gm/cm^3

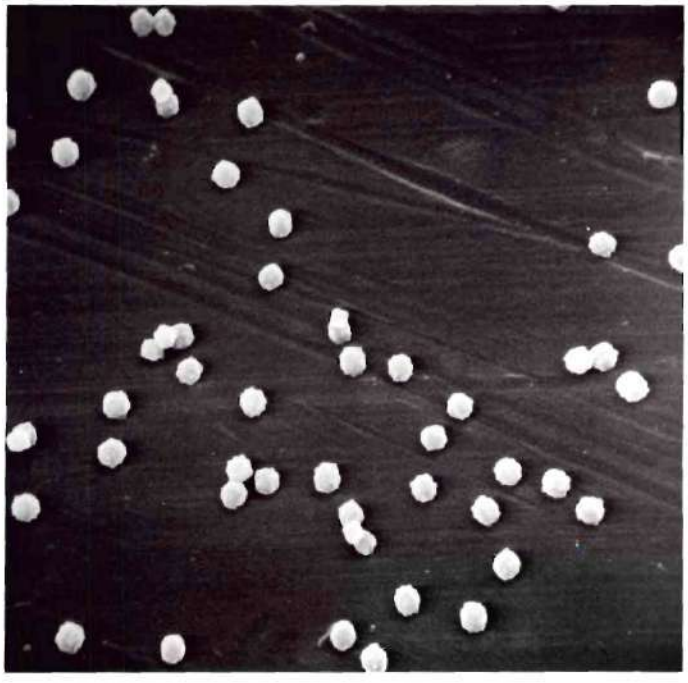

D_{St} = 1.09 μm

$\bar{\rho}$ = 1.50 gm/cm^3

Figure 6. Sodium Chloride Aerosol Particles

Magnification 4335 X

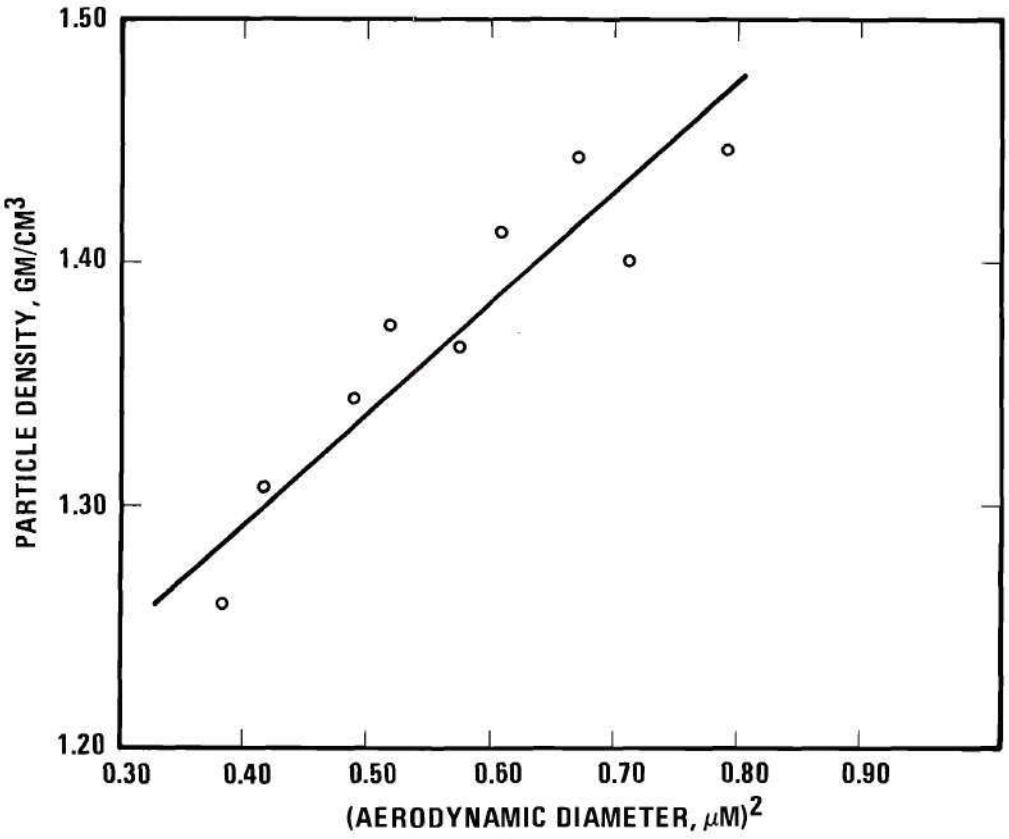

Figure 7. Particle Density as a Function of Aerodynamic Diameter Squared

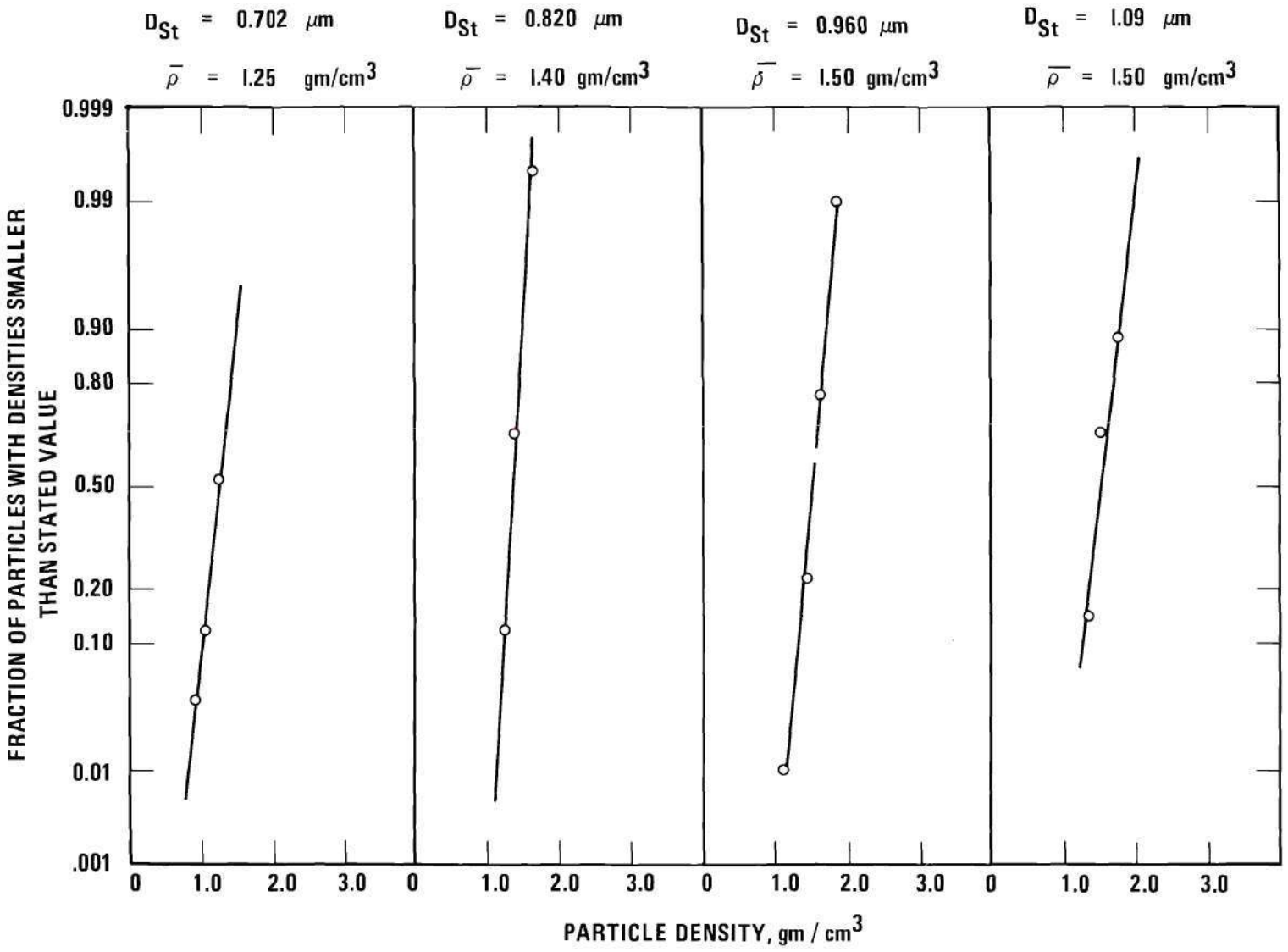

Figure 8. Cumulative Plot of Aerosol Particle Densities

diameter, and at higher flow rates the density deviations increased. This effect can be seen in Figure 9. The fact that the particle densities decrease with less time in the primary furnace supports the hypothesis that the aerosols are formed by the clustering of critical nuclei.

Relationship of Particle Density at Constant Flow Rate to Temperature

A primary consideration in the theory of the nucleation of the critical clusters is the temperature of the vaporizing chamber. As the temperature rises the particles should not only increase in aerodynamic diameter but should also increase in density. This is because at higher temperatures the kinetic energy of the system is higher, the randomness or absolute entropy of the system is greater, and there is less probability of an ordered group of clusters sticking together. The particles are larger due to higher vapor concentrations. The particles probably are formed more by addition of single nuclei than by large clusters. At a constant flow rate the effect of increasing the temperatures was found to increase mean particles densities. The results are shown in Figure 10.

Figure 10 shows only apparent trends in the relationships between density and flow rates and temperatures. No quantitative relationships should be drawn from these data.

Error Analysis

The error analysis for this research is divided in two sections, errors in the centrifuge calibration and errors in analysis of the sodium chloride aerosols.

1. The calibration curves were made using aerosols which for all practical purposes are monodisperse. Errors introduced in the centrifuge

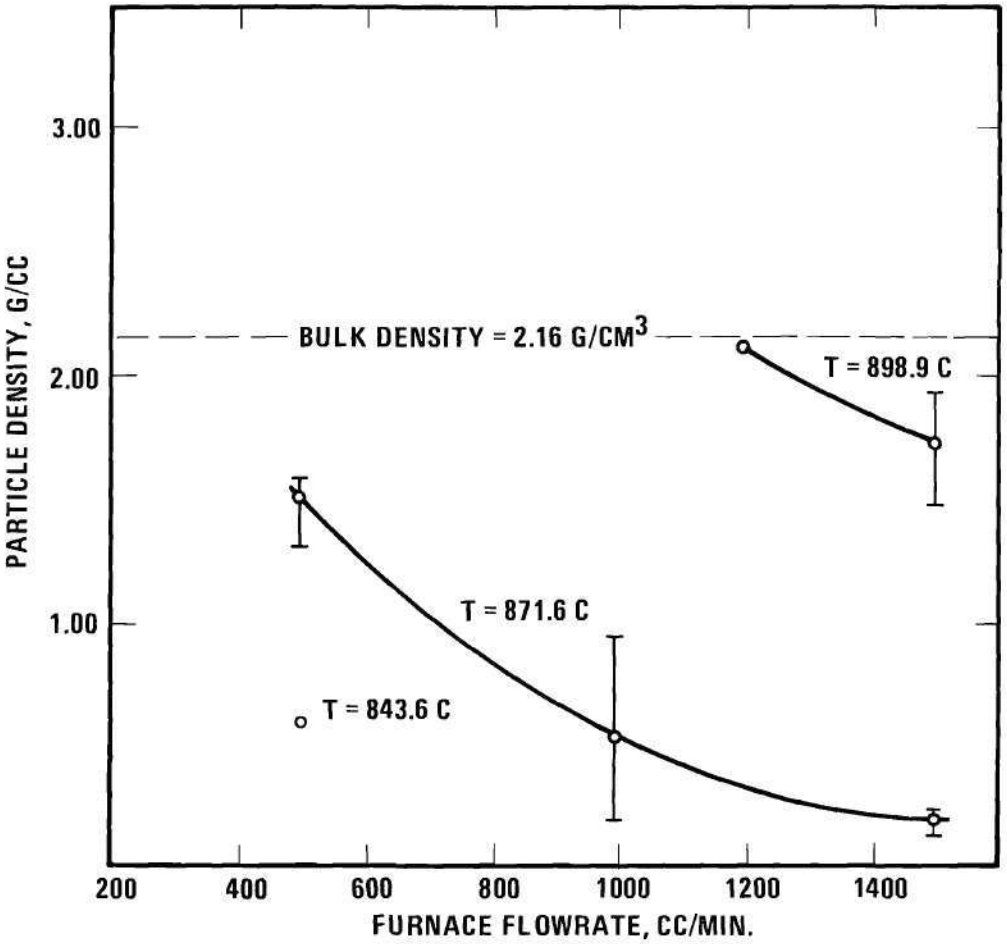

Figure 9. Particle Density as a Function of Flowrate

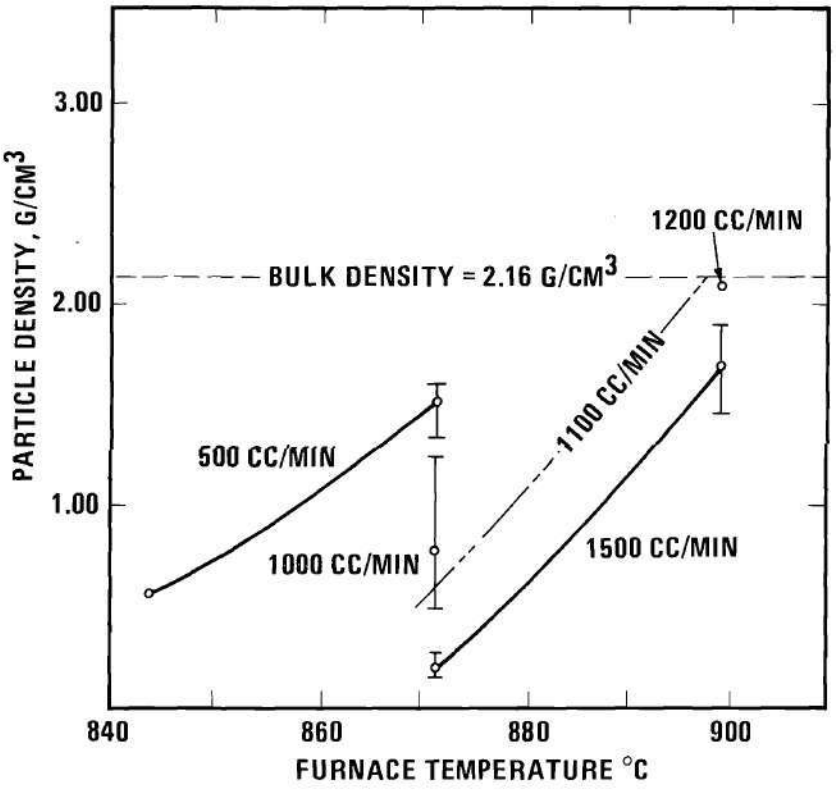

Figure 10. Particle Density as a Function of Temperature

calibration arise from the measurement of the sedimentation distance. The sedimentation distances could be measured to the nearest 0.5 mm which leads to an error of 1.25 percent.

2 A minute change in voltage to the centrifuge motor grossly affected the centrifuge speed. The centrifuge speed was controlled by constantly timing it with a strobe light. When the line voltage changed by $\pm$ 2.0 volts the centrifuge speed changed by 50 to 100 RPM, and the speed had to be reset. This had the effect of spreading the deposit on the foil and, because the centrifuge speed appears twice in the sedimentation equation--once to the second power and once exponentially to the second power--it is quite important. It is estimated that centrifuge speed changes introduced a $\pm$ 5.0 percent error.

3. The sodium chloride aerosols were all collected within the same time span after introduction of the crucible into the furnace. The mass concentration of sodium chloride appeared to decrease about 8.0 percent per hour after introduction of the sample. This obviously had an effect on particle size. The time interval over which the samples were taken after the crucible was placed in the furnace was approximately 2 hours. This would introduce an error in estimating the relationship of particle size to temperature and flow rate. A check of the aerodynamic particle diameter using the centrifuge showed that at 871°C particle size decreased approximately 10 percent in a four-hour period. No determination was made of the effect that overall time had on the density of the aerosol particles, but it was assumed that the effect would be to make the particles less dense because the concentration of vapor would be reduced from the first heater.

4. The assumption of two dimensional flow in the derivation of the sedimentation equation introduced errors by virtue of neglecting the effect of internal vortices. Since no method of measuring the magnitude of this error was available its effect is not quantified.

5. It will be noticed that in the determination of mean particle density, some of the calculations revealed densities greater than the bulk density of the material. This can be seen in the tables of Appendix B. It is attributed to the large standard deviations of diameters exhibited by some of the aerosol samples. The presence of these samples only reflects the non ideal conditions in the centrifuge and the presence of possible turbulence which tended to misplace the particles. It is also possible that the degree of monodispersity was not as great as it was believed to be at the time the sample was taken.

6. A quantitative analysis of the Tyndall spectra was attempted to reinforce the optical diameters measurements of the SEM. The attempt was unsuccessful due to the crude construction of the OWL. It was primarily useful as a qualitative instrument and permitted a determination of when the aerosol was monodisperse. The standard deviation of the optical diameters of the aerosol particles is a good indication of the degree of monodispersity of the aerosol. These results are tabulated in Appendix B. In general the standard deviation was between 10 and 30 percent of the mean optical diameter.

CHAPTER V

CONCLUSIONS

This research project was aimed at testing a modification of a Hochrainer aerosol centrifuge and applying that centrifuge to the study of density distributions in sodium chloride aerosols.

It is concluded that:

1. The modification of the Hochrainer centrifuge, that is using round holes instead of slits as channels for the aerosol to enter the annular channel, provides an improved method for determination of the aerodynamic diameters of aerosol particles.

2. The flow in the annular channel may be determined from a calibration of the exit orifice of the centrifuge.

3. The sedimentation distance for any size of aerosol particle which might enter the centrifuge can be calculated from Equation 6. This equation should prove quite useful in further centrifuge design.

4. Sodium chloride condensation aerosols have density distributions which deviate from the bulk density of the material. This is caused by the agglomeration of clusters in the aerosol generator.

5. The density deviation of sodium chloride aerosols is inversely related to the aerodynamic particle diameter.

6. Density deviations at fixed temperatures, which ranged from 843.6°C to 898.9°C, vary in a direct manner with the flow rate through the aerosol generator.

7. Density deviations at specific flow rates, which ranged from

500 cc/min to 1500 cc/min, vary in an inverse manner with the temperature in the primary heater of the aerosol generator.

CHAPTER VI

RECOMMENDATIONS

The Hochrainer centrifuge has been found to be an efficient tool in the determination of the aerodynamic diameter of particles primarily because of its ease of construction and the fact that discrete particle size separation can be obtained. Several additional modifications should be made to increase its utility. Since it was found that the trajectory of particles can be approximated with fair accuracy, specifications of a centrifuge to analyze any size spectrum of particles could be determined by the use of optimization techniques and a knowledge of the strength of materials of construction. This aerosol centrifuge design need not be limited to the size analysis of submicron particles only.

This type of centrifuge should be applied to the analysis of atmospheric particulate material as well as for the calibration of aerosol generating systems.

Further study of the phenomena of density distributions could be made with aerosols produced by methods other than condensation processes to determine if density distributions are present. The study of condensation aerosols should be continued using an aerosol which is not as hygroscopic as sodium chloride.

APPENDICES

APPENDIX A

AEROSOL CENTRIFUGE CALIBRATION DATA

Table 3. Calibration Data for Aerosol Centrifuge

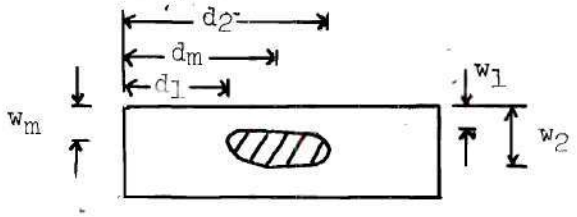

.0254 cm Orifice	(Distance in cm.)						
Particle Size (Microns)	d_1	d_2	d_m	w_1	w_2	w_m	Adjusted Particle Diameter According to Table 2
.822(s)	.90	1.0	.95	.2	.3	.25	.822
.822(d)	.70	.75	.72	.2	.3	.25	.970
.577(s)	1.60	1.80	1.70	.2	.3	.25	.577
.577(d)	1.22	1.29	1.25	.15	.3	.25	.680
.577(t)	1.00	1.10	1.05	.15	.3	.25	.767
.577(q)	.80	1.00	.90	.15	.25	.20	.845
.481(s)	1.60	1.90	1.75	.20	.30	.25	.481
.481(d)	1.35	1.40	1.38	.2	.30	.25	.567
.312(s)	2.80	3.00	2.90	.15	.35	.25	.312
.0342 cm Orifice							
1.1(s)	.7	.9	.80	.2	.3	.25	1.10
1.1(d)	.5	.65	.60	.2	.3	.25	1.30
.822(s)	1.45	1.60	1.50	.20	.30	.25	.822
.577(s)	2.45	2.75	2.60	.2	.35	.30	.577
.577(d)	2.00	2.25	2.10	.2	.3	.25	.680
.577(t)	1.55	1.75	1.60	.2	.3	.25	.767
.481(s)	2.80	3.00	2.90	.2	.4	.35	.481
.481(d)	2.20	2.40	2.30	.2	.3	.25	.567

Table 3. (Continued)

Particle Size (Microns)	d_1	d_2	d_m	w_1	w_2	w_m	Adjusted Particle Diameter According to Table 2.
.0406 cm Orifice							
1.30(s)	.90	1.10	.95	.2	.3	.25	1.30
1.30(d)	.70	.80	.75	.2	.3	.25	1.53
1.10(s)	1.00	1.15	1.10	.20	.30	.25	1.10
1.10(d)	.70	.90	.80	.20	.30	.25	1.30
.822(s)	2.00	2.200	2.10	.2	.3	.25	.822
.822(d)	1.40	1.60	1.50	.2	.3	.25	.970
.481(s)	2.90	3.20	3.10	.2	.3	.25	.481
.0508 cm Orifice							
1.30(s)	.90	1.00	.95	.2	.3	.25	1.30
1.30(d)	.70	.85	.75	.2	.3	.25	1.53
1.10(s)	1.00	1.25	1.10	.2	.3	.25	1.10
1.10(d)	.80	.95	.87	.2	.3	.25	1.30
.822(s)	1.85	2.10	1.95	.17	.35	.26	.822
.822(d)	1.35	1.60	1.45	.15	.30	.25	.970
.822(t)	1.10	1.30	1.20	.20	.30	.25	1.09
.481(s)	3.10	3.50	3.30	.2	.3	.25	.481
.481(d)	2.50	2.75	2.67	.2	.3	.25	.567
.481(t)	2.10	2.30	2.20	.2	.3	.25	.640
.481(q)	1.90	2.20	1.95	.20	.22	.21	.700

(s) singlet
(d) doublet
(t) triplet
(q) quadruplet

APPENDIX B

TABULATION OF EXPERIMENTAL RESULTS OF SODIUM CHLORIDE AEROSOL DENSITY ANALYSIS

Table 4. Sodium Chloride Aerosol Analysis Data

Temperature: 871.9°C

Flowrate: 500 cc/min

Aerodynamic Dia. : .960 μm

Frequency	2	32	81	32	2
Optical Diameter (DO)	.636	.700	.760	.815	.875
Density G/cm^3	2.27	1.88	1.59	1.38	1.20

$\overline{DO}$ .758 ± .082

ρ 1.61 ± .372

Temperature: 871.9°C

Flowrate: 500 cc/min

Aerodynamic Dia. 1.09 μm

Frequency	2	4	10	25	7
Optical Diameter (DO)	.71	.772	.831	.891	.950
Density G/cm^3	2.35	1.99	1.72	1.49	1.32

$\overline{DO}$ = .869 ± .125

ρ = 1.59 ± .510

Table 4. (Continued)

Temperature: 871.9°C

Flowrate: 500 cc/min

Aerodynamic Dia. : .702 μm

Frequency	11	10	2	1
Optical Diameter (DO)	.576	.636	.700	.760
Density G/cm^3	1.47	1.21	1.00	.848

$\overline{DO}$ .619 $\pm$ .094

ρ 1.29 $\pm$ .358

Temperature: 871.9°C

Flowrate: 500 cc/min

Aerodynamic Dia. : .820 μm

Frequency	1	35	63	14
Optical Diameter (DO)	.576	.636	.700	.760
Density G/cm^3	2.02	1.66	1.37	1.16

$\overline{DO}$ = .686 $\pm$ .074

ρ = 1.40 $\pm$ .325

Table 4. (Continued)

Temperature: 871.9°C

Flowrate: 1000 cm^3/min

Aerodynamic Dia. : 1.42 μm

Frequency	10	14	18	5	4	5	1
Optical Diameter (DO)	1.22	1.35	1.48	1.60	1.73	1.86	1.99
Density G/cm^3	1.35	1.10	.92	.787	.673	.582	.509

$\overline{DO}$ 1.47 ± .464

ρ .973 ± .568

Temperature: 871.9° C

Flowrate: 1000 cm^3/min

Aerodynamic Dia. 2.40 μm

Frequency	1	5	4	24	9	6	3	4
Optical Diameter (DO)	2.45	2.70	2.96	3.22	3.46	3.72	3.98	4.23
Density G/cm^3	.959	.790	.657	.555	.481	.416	.363	.321

$\overline{DO}$ 3.34 ± 1.06

ρ .536 ± .340

Table 4. (Continued)

Temperature: 871.9°C

Flowrate: 1000 cm^3/min

Aerodynamic Dia. : 1.58 μm

Frequency	1	3	7	9	11	16	7	2	2
Optical Diameter (DO)	2.45	2.7	2.96	3.22	3.46	3.72	3.98	4.23	4.5
Density G/cm^3	.415	.342	.284	.240	.208	.180	.157	.139	.123

$\overline{DO} = 3.50 \pm 1.25$

$\rho = .213 \pm .162$

Temperature: 898.9°C

Flowrate: 1500 cc/min

Aerodynamic Dia. : 1.37 μm

Frequency	16	77	32
Optical Diameter (DO)	.84	.99	1.12
Density G/cm^3	2.66	1.915	1.49

$\overline{DO}$ $1.004 \pm .128$

ρ $1.90 \pm .492$

Table 4. (Continued)

Temperature: 898.9°C

Flowrate: 1500 cc/min

Aerodynamic Dia. : 1.10 μm

Frequency	4	48	48	2
Optical Diameter (DO)	.72	.84	.99	1.12
Density G/cm^3	2.33	1.71	1.23	.964

$\overline{DO} = .9114 \pm .170$

$\rho = 1.494 \pm .572$

Temperature: 898.9°C

Flowrate: 1200 cc/min

Aerodynamic Dia. 2.8 μm

Frequency	1	7	2	14	35	25	6
Optical Diameter (DO)	1.38	1.52	1.66	1.81	1.95	2.09	2.23
Density G/cm^3	4.11	3.39	2.84	2.39	2.06	1.79	1.57

$\overline{DO}$ $1.93 \pm .432$

ρ $2.12 \pm .934$

Table 4. (Continued)

Temperature: 898.9°C

Flowrate: 1200 cc/min

Aerodynamic Dia. :2.45 μm

Frequency	4	20	38	24	7
Optical Diameter (DO)	1.39	1.54	1.68	1.83	1.95
Density G/cm^3	3.1	2.53	2.12	1.79	1.57

$\overline{DO} = 1.697 \pm .285$

$\rho = 2.123 \pm .718$

Temperature: 843.6°C

Flowrate: 500 cc/min

Aerodynamic Dia. : .66 μm

Frequency	11	5	4
Optical Diameter (DO)	.76	.85	.95
Density G/cm^3	.754	.60	.482

$\overline{DO} = .821 \pm .12$

$\rho = .662 \pm .184$

Table 4. (Continued)

Temperature: 871.6°C

Flowrate: 500

Aerodynamic Dia. : .62 μm

Frequency	2	27	62	8
Optical Diameter (DO)	.448	.506	.564	.622
Density G/cm^3	1.915	1.50	1.20	.99

$\overline{DO}$ $.550 \pm .07$

ρ $1.279 \pm .352$

Temperature: 871.6°C

Flowrate: 500

Aerodynamic Dia. : .70 μm

Frequency	1	12	54	38	14
Optical Diameter (DO)	.448	.506	.564	.622	.681
Density G/cm^3	2.44	1.91	1.54	1.26	1.05

$\overline{DO}$ $.589 \pm .106$

ρ $1.44 \pm .0863$

Table 4. (Continued)

Temperature: 871.6°C

Flowrate: 500

Aerodynamic Dia. .65 μm

Frequency	1	24	48	17	2
Optical Diameter (DO)	.448	.506	.564	.622	.681
Density G/cm^3	2.1	1.65	1.32	1.09	.91

$\overline{DO} = .560 \pm .086$

$\rho = 1.37 \pm .023$

Temperature: 871.6 ℃

Flowrate: 500 cc/min

Aerodynamic Dia. : .76 μm

Frequency	1	27	107	37	3
Optical Diameter (DO)	.506	.564	.622	.681	.739
Density G/cm^3	2.25	1.81	1.49	1.24	1.05

$\overline{DO}$ $.627 \pm .077$

ρ $1.483 \pm .361$

Table 4. (Continued)

Temperature: 871.6°C

Flowrate: 500 cm^3/min

Aerodynamic Dia. : .72 μm

Frequency:	5	48	57	30	4	1
Optical Diameter (DO)	.506	.564	.622	.681	.739	.973
Density G/cm^3	2.02	1.62	1.34	1.11	.95	.547

$\overline{DO} = .616 \pm .133$

$\rho = 1.402 \pm .029$

Temperature: 871° C

Flowrate: 500 cc/min

Aerodynamic Dia. : .82 μm

Frequency	1	39	90	81	20	1
Optical Diameter (DO)	.506	.564	.622	.681	.739	.797
Density G/cm^3	2.62	2.11	1.73	1.44	1.23	1.08

$\overline{DO}$ $.6432 \pm .115$

ρ $1.646 \pm .525$

Table 4. (Continued)

Temperature: 871°C

Flowrate: 500 cc/min

Aerodynamic Dia. : .78 μm

Frequency	1	34	87	34	3
Optical Diameter (DO)	.506	.564	.622	.681	.739
Density G/cm^3	2.37	1.91	1.57	1.31	1.11

$\overline{DO} = .623 \pm .0807$

$\rho = 1.574 \pm .019$

Temperature: 871°C

Flowrate: 500 cm/min

Aerodynamic Dia. : .890 μm

Frequency	5	25	54	41	10	4
Optical Diameter (DO)	.569	.628	.688	.746	.805	.863
Density G/cm^3	2.42	2.02	1.67	1.42	1.22	1.08

$\overline{DO}$ $.703 \pm .145$

ρ $1.636 \pm .054$

Table 4. (Concluded)

Temperature: 871.6°C

Flowrate: 500 cm^3/min

Aerodynamic Dia. : .85 μm

Frequency	1	8	64	94	59	13	3
Optical Diameter (DO)	.511	.569	.628	.688	.746	.805	.863
Density G/cm^3	2.81	2.25	1.82	1.53	1.30	1.12	.970

$\overline{DO} = .690 \pm .1405$

$\rho = 1.55 \pm .024$

APPENDIX C

THE DERIVATION OF THE PRESSURE DROP EXPRESSION THROUGH THE CENTRIFUGE ORIFICE AND CALCULATION OF THE AVERAGE ANNULAR GAS VELOCITY IN THE ANNULAR CHANNEL

The following assumptions are made to facilitate the calculations:

1. The exit orifice limits the flow in the channel.
2. The channel curvature does not significantly affect the velocity patterns.
3. The flow is laminar at all times with no secondary flow.
4. The carrier gas is pure nitrogen.
5. The flow is isothermal.

The pressure drop across the orifice will be considered entirely due to the centrifugal force field and it will be assumed that the pressure is one atmosphere both at the center of the centrifuge and at the exit side of the orifice. The change in pressure radially across the channel is:

$$\frac{dP}{dR} = \frac{d}{dR}\left(\frac{F(R)}{A(R)}\right) = \frac{1}{A^2}\left[A\,\frac{dF}{dR} - F\,\frac{dA}{dR}\right] \qquad \text{(C-1)}$$

The total area across which the force field is changing is:

$$A = 2\pi Rh \qquad \text{(C-2)}$$

Let $h = 1.0$, for a unit height.

If an infinitely small mass of gas is subjected to the force

field, the force will be

$$F = mR\omega^2 \tag{C-3}$$

$$\frac{dF}{dR} = m\omega^2 + R\omega^2 \frac{dm}{dR} \tag{C-4}$$

Therefore, combining equations C-1, C-2 and C-4 it can be shown that

$$\frac{dP}{dR} = \frac{\omega^2}{2\pi} \frac{dm}{dR} \tag{C-5}$$

if

$$\frac{dm}{dR} = \rho g \frac{dV}{dR} \tag{C-6}$$

and

$$\rho g = \rho g(R) \tag{C-7}$$

$$\frac{dV}{dR} = 2\pi R \tag{C-8}$$

$$\frac{dP}{dR} = \omega^2 \rho g(R) R \tag{C-9}$$

For isothermal conditions

$$\rho g(R) = \frac{P(R)M}{R'T} \tag{C-10}$$

then

$$\frac{dP}{dR} = \frac{\omega^2 P(R) R}{R'T} \tag{C-11}$$

$$\frac{P}{P_o} = \exp\left(\frac{\omega^2 MR^2}{R'T}\right) \tag{C-12}$$

Assuming the following conditions:

R = 1.73 cm

ω = 1050 sec^{-1}

M = 28.00 gm/gm-mole

T = 300 K

$$\frac{P}{P_o} = 1.00187 \quad P_o = 1atm \tag{C-12}$$

or

$$\Delta P = 1695 \text{ dynes/cm}^2 \tag{C-14}$$

Then using equation C-15 the flow through a perfect orifice plate can be found for this pressure drop

$$Q = C_\Delta A_o \rho_g \sqrt{-2\rho g \Delta P} \tag{C-15}$$

Values of the experimental and theoretical flows are listed in Table C-1 for average channel flow velocity which is found by dividing the volume flow rate through the orifice by the cross sectional area of the annular channel.

Table 5. Comparison of Experimentally Measured and Calculated Gas Flow Through Centrifuge Orifices

Orifice Diameter (cm)	Pressure Drop Across Orifice (Dynes/cm)	Average Channel Velocity (cm/sec)	
		Calculated	Experimental
0.0254	255	1.39	.318
	1275	3.12	3.64
	1695	3.60	4.90
	2250	4.42	6.50
0.0342	255	2.51	.900
	1275	5.61	5.89
	1695	6.46	7.25
	2250	7.94	9.02
0.0406	255	3.58	3.90
	1275	8.01	10.01
	1695	9.22	11.97
	2250	11.93	14.76
0.0508	255	5.59	3.44
	1275	12.51	9.12
	1695	14.41	10.94
	2250	17.70	13.84

APPENDIX D

COMPARISON OF SEDIMENTATION LENGTH FUNCTIONS

The Fuchs-Stechina correction (14) to Stokes' law was used to calculate the radial terminal velocity of the particle. It may be written

$$F = \frac{-3\pi\eta D_{AE} V_s(R)}{\frac{1}{1+\beta x} + \frac{2.25x}{\delta}} \tag{D-1}$$

From consideration that the particle is in a centrifugal force field

$$F = \frac{\pi D_{ae}^2 \rho \omega^2 R}{8} \tag{D-2}$$

This yields

$$V_s(R) = \frac{DO^2 \rho \omega^2 R}{18\eta} \left[\frac{1}{1+\beta x} + \frac{2.25x}{\delta}\right] \tag{D-3}$$

All values in equation D-3 are design constants of the centrifuge and surroundings except D_{ae} and R so it can be said that

$$V_s(R) = (A')\ (R) \tag{D-4}$$

$$A = \frac{DO^2 \rho \omega^2}{18\eta}\left[\frac{1}{1+\beta x} + \frac{2.25x}{\delta}\right] \tag{D-5}$$

$$\frac{dR}{dt} = A'R \tag{D-6}$$

and

$$R = ae^{A't} \tag{D-7}$$

From Goldstein (13) the velocity distribution in the angular or z direction in the annulus is described by equation D-8 and D-9. The pressure gradient in the radial direction has also been considered herein

$$W = -\frac{1}{2\eta}\frac{d\rho}{d\theta}\left[\frac{b^2\log b - a^2\log a}{(b^2-a^2)}R - \frac{a^2b^2}{(b^2-a^2)}(\log\frac{b}{a})\frac{1}{R} - R\log R\right] \qquad (D\text{-}8)$$

$$\bar{w} = -\frac{1}{2\eta}\frac{d\rho}{d\theta}\left(\frac{1}{b-a}\right)\left[\frac{(b^2-a^2)}{4} - \frac{a^2b^2}{(b^2-a^2)}(\log\frac{b}{a})^2\right] \qquad (D\text{-}9)$$

The particle velocity is assumed to be identical to the gas stream velocity. $\bar{w}$ can be found from the experimental results presented in Appendix C. This allows calculation of the pressure gradient term $-\frac{1}{2\eta}\frac{\partial\rho}{\delta\theta}$. Integration of equation D-8 with substitution of equation D-7 for R yields as the final trajectory formula for any particle

$$Z = \left[\frac{(b-a)\bar{w}}{\frac{b^2-a^2}{4} - \frac{a^2b^2}{b^2-a^2}(\log b/a)^2}\right]\left[\frac{D_o^2\rho\omega^2}{18\eta}\left(\frac{1}{1+\beta x} + \frac{2.25x}{\delta}\right)\right]\left[\frac{b^2\log b - a^2\log a}{b^2-a^2}a\left(\frac{b}{a}-1\right) + \left(\frac{a}{b}-1\right)\frac{ab^2}{b^2-a^2}\right.$$

$$\left.(\log b/a) + a\left(\frac{b}{a}-1\right) - a\left(\frac{b}{a}\{\log\frac{b}{a}-1\}+1\right)\right] \qquad (D\text{-}10)$$

For equation D-10 all values are design constants except $\bar{w}$ and D_o. The resulting equation for the centrifuge used in this research is

$$Z = \frac{\bar{w}}{A},\ (.329) \qquad (D\text{-}11)$$

An alternate method of estimating sedimentation distance is to assume plug flow in the annulus and use the log mean radial velocity to

estimate the trajectory time. From equation D-6 the average time to cross the channel is

$$t = \frac{1}{A'} \ell n(b/a) \tag{D-12}$$

Integrating the average velocity in the z direction over the time yields for the sedimentation distance

$$Z = \int_0^{\frac{1}{A}\ell nb/a} \bar{w}\, dt = \frac{\bar{w}}{A} \ell n(b/a) \tag{D-13}$$

It so happens that this second approximation gives results very close to those predicted from equation D-10. Although the average velocity (radial) term gives good results in this case it should not be used indiscriminately.

The sedimentation distances calculated for each orifice and each particle diameter of calibration aerosol are listed in Table 6. A comparison of these values with the experimental values is shown in Figures 5a-d.

Table 6. Calculated Sedimentation Distances for Different Orifices

Particle Diameter (ρ=1) μm	Orifice Diameter (cm)/Gas Velocity (cm/sec)			
	0.0254/4.9	0.0342/7.25	0.0406/11.97	0.0508/10.94
1.1	.328	.485	.801	.732
.822	.563	.833	1.37	1.25
.481	1.504	2.22	3.67	3.35
.312	3.82	5.66	9.34	8.54

APPENDIX E

NOMENCLATURE

$V_s(R)$	sedimentation terminal velocity. (cm/sec)
DAE	Aerodynamic diameter (μm)
DO	Optical diameter (μm)
ρ	Particle Density (gm/cc)
ρg	carrier gas density (gm/cc)
g	gravitational force constant (980 cm/sec^2)
C	Any correction factor for particle sedimentatation. (dimensionless)
Z	Sedimentation distance (cm)
Q	Volume flow rate (cc/sec)
a	inner wall of annular channel (cm)
b	outer wall of annular channel (cm)
ω	angular velocity of centrifuge (sec^{-1})
$\bar{w}$	average annular gas velocity (cm/sec)
w	annular gas velocity (cm/sec)
A	Cunninghams correction to Stokes Law (dim.)
A'	Combined Fuchs-Stechina correction factor (sec^{-1})
R	radial position of a particle in centrifuge (cm)
β	0.42 (dimensionless)
δ	1.35 (dimensionless)
X	$2/D_{st}$ (dimensionless)

λ mean free path length of gas molecule (6.53×10^{-6} cm)

F force on the particle system ($gm/cm^2\text{-}sec^2$)

A_o orifice cross section (cm^2)

η gas viscosity (gm/cm-sec)

P gas pressure ($dynes/cm^2$)

LITERATURE CITED

1. V. K. Lamer, E. C. Y. Inn and I. B. Wilson, The Methods of Forming; Detecting, and Measuring the Size and Concentration of Liquid Aerosols in the Size Range of .01μm to .25μm Diameter, Journal of Colloid Science 5, 471-496, 1950.

2. M. J. Matteson, J. J. Fox and O. Preining, The Density Distributions of Sodium Chloride Aerosols Formed by Condensation, Nature, 238, 61, 1972.

3. O. R. Moss, H. H. Ettinger and J. R. Coulter, Aerosol Density Measurements using a Modified Spiral Centrifuge Aerosol Spectrometer, Environmental Science and Technology, 6, No. 7, 614-17, 1972.

4. R. C. Weast, S. M. Selby and C. D. Hodgman, Handbook of Chemistry and Physics, 45th Ed., Chemical Rubber Company, Cleveland, Ohio, P B221, 1965.

5. F. Stein, N. Esmen and M. Corn, The Density of Uranine Aerosol Particles, American Industrial Hygiene Journal, 27, No. 1, 428-430, 1966.

6. M. I. Tillery and M. G. McKnight, On the Density of Uranine Particles, American Industrial Hygiene Journal, 28, No. 9, 491, 1967.

7. G. A. Sehmel, The Density of Uranine Particles Produced by a Spinning Disc Aerosol Generator, American Industrial Hygiene Journal, 28, No. 9, 498-9, 1967.

8. D. Hochrainer, A New Centrifuge to Measure the Aerodynamic Diameter of Aerosol Particles in the Submicron Range, Journal of Colloid and Interface Science, 36, No. 2, 191-94, 1971.

9. J. M. Coulson and J. F. Richardson, Chemical Engineering, 2nd. ed., Pergamon Press, New York, p. 112, 196.

10. H. L. Green and W. R. Lane, Particulate Aerosols; Dusts, Smoke, and Mists, 2nd. Ed., E. and F. N. Spoon, London, England, 1964.

11. O. Preining, Zum Problem der Eichung Fraktionierender Mebgerate fur Staube der Korngroben Zwishen 0.1 und 1.0 Mikron mit Hilfe von Testaerosolen, Staub, 22, No. 11, 456-63, 1962.

12. W. Stober, A. Berner and R. Blascheke, The Aerodynamic Diameter of Aggregates of Uniform Spheres, Journal of Colloid and Interface Science, 29, No. 4, 710-19, 1969.

13. S. Goldstein, Modern Developments in Fluid Mechanics, 1st ed. Clarendon Press, Oxford, England, Vol I., 1938, p. 316.

14. N. A. Fuchs and I. B. Stechnia, Resistance of a Gaseous Medium to the Motion of a Spherical Particle of a Size Comparable to the Mean Free Path of the Gas Molecules, Transactions of the Faraday Society, 58, No. 1, 1949-52, 1962.